Parametric Modeling for Curved Slots of Vivaldi Antenna Based on Artificial Neural Network

Wen-Hao Su[1], Wei Shao[1], Haiyan Ou[1], and Sheng-Jun Zhang[2]

[1]School of Physics
University of Electronic Science and Technology of China, Chengdu, 611731, China
suwenhao1202@163.com, weishao@uestc.edu.cn, ouhaiyan@uestc.edu.cn

[2]National Key Laboratory of Science and Technology on Test Physics and Numerical Mathematics
Beijing, 100076, China
zhangsj98@sina.com

Abstract – This paper proposes an artificial neural network (ANN) model based on parametric modeling for curved slots of the Vivaldi antenna. A more effective processing method is achieved by feeding ANN with the point positions that produce curved edges via cubic spline interpolation rather than the picture of metallic patches. The predicted results of ANN, including *S*-parameter and gain, agree well with those from the full-wave simulation. With the trained model, a Vivaldi antenna with the lower cut-off frequency is optimized by the multi-objective genetic algorithm.

Index Terms – Artificial neural network, cubic spline interpolation, parametric modeling, Vivaldi antenna.

I. INTRODUCTION

Vivaldi antennas have been widely used in many ultra-wideband (UWB) applications such as ground penetrating radar [1], detection [2], communication [3], etc. The Vivaldi antenna was first introduced by Gibson in 1979 [4], while Gazit later proposed the antipodal Vivaldi antenna (AVA) in 1988 [5]. To reduce cross-polarization, Langley designed the balanced Vivaldi antenna (BAVA) [6]. With the improvement of equipment integration, BAVA needs to provide outstanding performance in a limited size. As a miniaturization approach, different types of corrugations have been extensively used in the design of BAVA. Corrugation refers to repetitive, evenly spaced and identical shaped slots made on the outer flare edge which coincides with the edge of the substrate. Corrugation helps to extend the current path to improve the bandwidth of BAVA. The current slot design, however, relies on some relatively simple curves, such as straight lines [7], elliptic curves [8], and exponential curves [9]. These curves cannot be changed arbitrarily, which constrains the design freedom of slots, leading to a limited radiation performance. More crucially, the structure of BAVA is composed of a number of curves, which will definitely increase the calculation time due to the small-grid division in the electromagnetic (EM) full-wave simulation algorithm.

In recent years, it has been demonstrated that the artificial neural network (ANN) may replace the role of full-wave simulation in the process of antenna optimization [10–11]. In parametric modeling of neural networks, the input is the parameter values of the antenna structure, and the EM response serves as the output. An ANN model with three parallel and independent branches has been presented to describe three different performance indexes of the Fabry–Perot resonator antenna [12]. Once the geometric parameters are input to the trained model, it can simultaneously predict *S*-parameter, gain, and radiation pattern. [13] presents an inverse ANN for the modeling of the multimode resonant antenna, where the input is the performance indexes, and the output is a set of related geometric parameters. The inverse model can provide antenna geometries directly without being repetitively called by an optimization process. Although ANN based on parametric modeling can effectively map the relationship from the input to the output, it is challenging to further improve the EM performance of an antenna due to its fixed topology structure using ANN.

[14] proposes a non-parametric modeling method for microwave filters using the convolutional neural network (CNN). Instead of the structural parameter values, the image of metallic patches is employed as the input of the neural network. Although the CNN model can change the component geometry flexibly and expand the solution domain, the structure of CNN is relatively complex, and the hyper-parameters in CNN are difficult to determine due to their huge number. Moreover, a large number of samples based on pixel images are required for CNN training, resulting in a time-consuming training process.

Submitted On: February 27, 2023
Accepted On: June 13, 2023

https://doi.org/10.13052/2023.ACES.J.380903

1054-4887 © ACES

In this paper, we propose an effective ANN for the parametric modeling of curved slots of BAVA. The structural parameters of a curved slot are used as the input of the model, including the longitudinal movement value of the points, rotation angle, slot width and length, while the output is the *S*-parameter and the gain of the antenna. The cubic spline interpolation method is used to generate curved slots, and the corresponding antenna structures are input to the CST software for simulation to provide training samples for ANN. After training, the ANN prediction results are in good agreement with the CST full-wave simulation results. The resulting BAVA can obtain wider bandwidth thanks to the multi-objective optimization of the non-dominated sorting genetic algorithm-II (NSGA-II), which repeatedly calls the trained ANN.

II. PROPOSED MODEL

In this paper, the curved slots shaped by ANN are introduced to extend the current path effectively. The training process of the proposed ANN model based on parametric modeling of BAVA is shown in Fig. 1. The geometric structure of a curved slot includes the longitudinal movement value of the points, rotation angle, slot width, and length. Based on cubic spline interpolation, a curve passing through these points is formed. Through translation and rotation, curves form a slot structure. The slot generated by the proposed ANN is repeatedly copied to produce corrugation in BAVA flares. The BAVA with corrugation is sent to the CST software for calculation, and the obtained *S*-parameters and gain at each frequency point are used to train the ANN. As the *S*-parameter has large fluctuations in the frequency band, 200 points are sampled evenly across the frequency band instead of vector fitting based on the transfer function. To simplify the neural network structure and speed up training, four sub-ANNs are trained with 50 sampling points each. Finally, the outputs of the four sub-ANNs, including ANN_1, ANN_2, ANN_3, and ANN_4, are combined to produce a complete *S*-parameter. ANN_5 is used to train the gain.

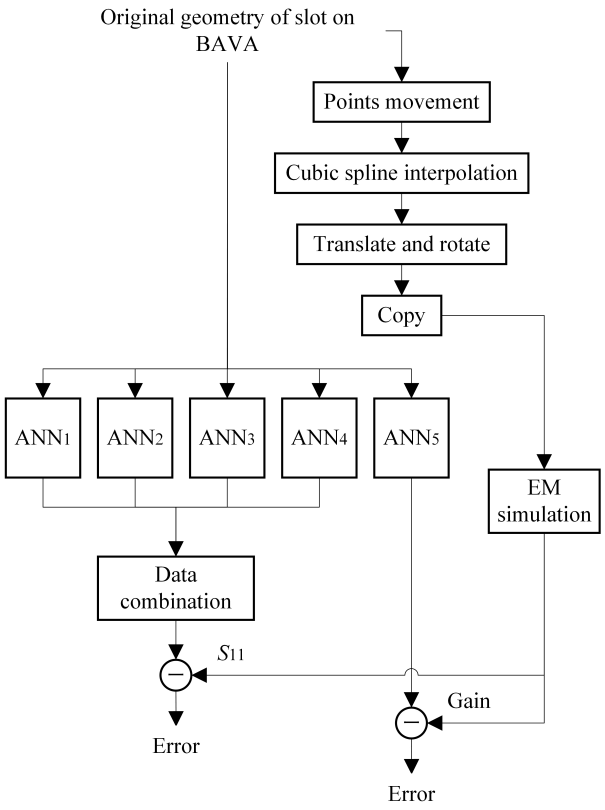

Fig. 1. Structure of the proposed model.

Cubic spline interpolation is applied to the modeling of the curved slots on the flares of BAVA, as shown in Fig. 2.

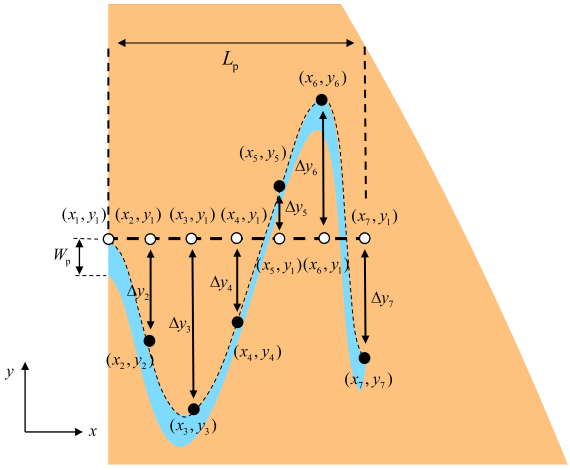

Fig. 2. Diagram of the parametric modeling for curves.

The length of the slot along the x direction is controlled by L_p. For example, seven points are set on the curve, and the position of the kth point is denoted by (x_k, y_k). The amount of space between any two adjacent points along the x-axis is the same. The first point is fixed at (x_1, y_1), and the remaining six points are moved along the y direction to control the curve shape of the slot. As a result, the curve consists of six piecewise curves. The cubic spline interpolation formula for the interval of $x_k \le x \le x_{k+1}$ is as follows

$$f(x) = y_k + \left[\frac{y_{k+1}-y_k}{x_{k+1}-x_k} - \frac{x_{k+1}-x_k}{2}m_k - \frac{x_{k+1}-x_k}{6}(m_{k+1}-m_k)\right](x-x_k) + \frac{m_k}{2}(x-x_k)^2 + \frac{m_{k+1}-m_k}{6(x_{k+1}-x_k)}(x-x_k)^3, k = 1,2,\ldots,6 \quad (1)$$

The corresponding linear equations for $m_1, m_2, \ldots,$ and m_k can be written as

$$\begin{bmatrix} 2 & 1 & & & \\ 1 & 4 & 1 & & \\ & \ddots & \ddots & \ddots & \\ & & 1 & 4 & 1 \\ & & & 1 & 2 \end{bmatrix} \begin{bmatrix} m_1 \\ m_2 \\ \vdots \\ m_k \\ m_{k+1} \end{bmatrix} = \frac{6}{h} \begin{bmatrix} \frac{y_2-y_1}{x_2-x_1} \\ \frac{y_3-y_2}{x_3-x_2} - \frac{y_2-y_1}{x_2-x_1} \\ \vdots \\ \frac{y_{k+1}-y_k}{x_{k+1}-x_k} - \frac{y_k-y_{k-1}}{x_k-x_{k-1}} \\ -\frac{y_{k+1}-y_k}{x_{k+1}-x_k} \end{bmatrix}, \quad (2)$$

where $h = L_p/6$. Once m_k are solved from (2), one edge of the curved slot can be obtained based on (1). Then, the curve is shifted along the y direction by the slot width of W_p to obtain the other edge of the slot. With the above operation, the shape change of the slot is achieved through the parametric modeling.

III. APPLICATION EXAMPLE

A BAVA [15] without the slot in Fig. 3 (a) is employed as an example to evaluated the proposed model. The BAVA consists of two substrate layers and three copper layers. The first and third copper layers connected by two metallic via holes serve as ground layers, and the middle layer acts as a conductor. All copper layers are separated by substrates. The original geometric parameters are as follows: L = 59.9 mm, L_1 = 22 mm, L_2 = 10 mm, L_3 = 10 mm, L_4 = 4 mm, W_a = 1 mm, W_g = 6.578 mm, W = 24 mm, W_{ms} = 0.4 mm, W_{sl} = 0.74 mm, and D_{vh} = 0.6 mm.

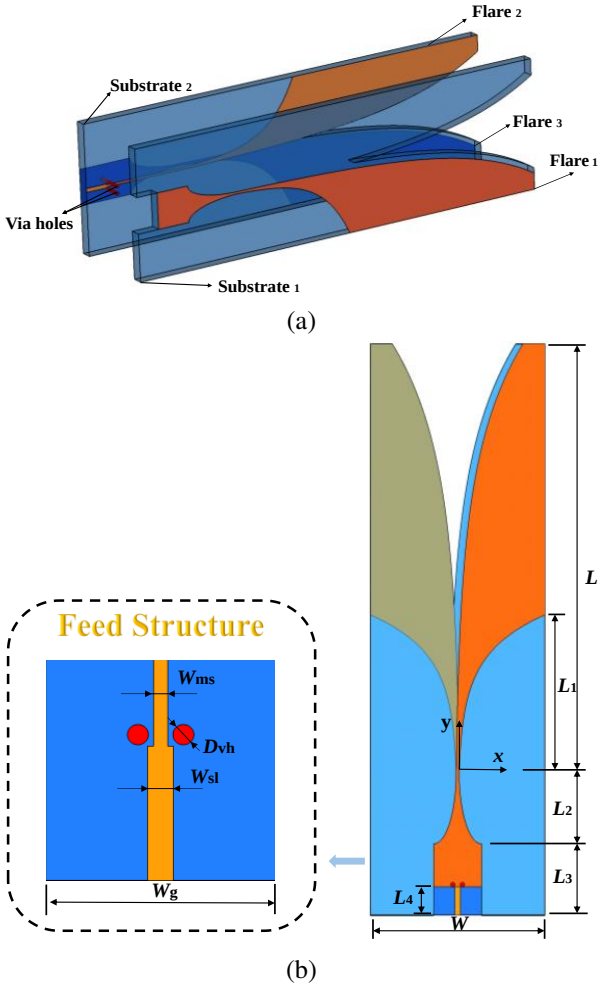

Fig. 3. Geometry of a BAVA without slots: (a) 3D view and (b) 2D view.

As shown in Fig. 3 (b), the inner and outer curved edge profiles of the flares are determined by [15]

$$\begin{cases} X_{\text{inner}} = \pm\left[-W_{ms} + (W_{ms}/2)\, e^{p_1 y}\right] \\ X_{\text{outer}} = \pm\left[(W_{ms}/2)\, e^{p_2 y}\right] \end{cases} \quad (3)$$

where p_1 = 0.064276 and p_2 = 0.157475. The asymmetric substrate cutout profile is then defined as

$$\begin{cases} X_1 = +\left[-W_{ms} + (W_{ms}/2)\, e^{p_1 y}\right] - W_a \\ X_2 = -\left[-W_{ms} + (W_{ms}/2)\, e^{p_1 y}\right] \end{cases}. \quad (4)$$

The metallic patch is printed on the substrate with a thickness of 0.254 mm and a relative dielectric constant of 2.2. Based on parametric modeling, the curved slots are introduced into the flares of BAVA. L_{up} is the distance between the slot and the top of flare, which is fixed at 3 mm. To increase the design freedom, a rotation angle is used as another variable of the slot structure as depicted in Fig. 4.

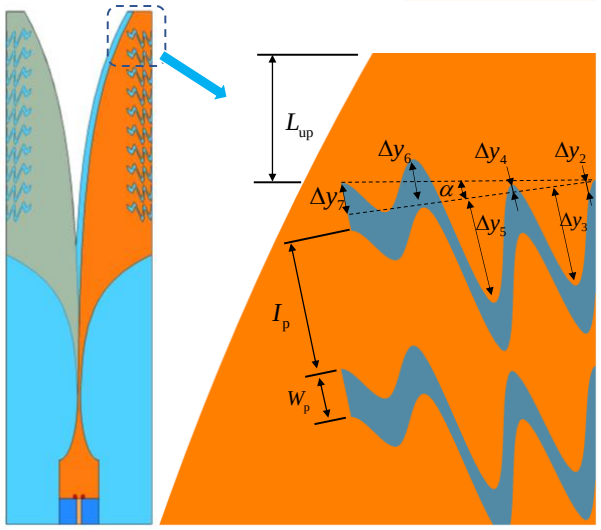

Fig. 4. Geometry of the curved slots.

The inputs of the proposed ANN model and their variation ranges are shown in Table 1, where Δy_k is the longitudinal movement of kth $(k = 2, 3, \cdots, 7)$ point, W_p and L_p represent the width and length of the slots, respectively, and α is the rotation angle of the slots. The design of experiment (DOE) method is used to collect 200 training samples and 50 testing samples.

Table 1: Definition of training and testing samples for the antenna

	Training Data (200 Samples)			Testing Data (50 Samples)		
	Min	Max	Step	Min	Max	Step
Δy_k (mm)	-1.7	1	0.3	-1.7	1	0.3
W_p(mm)	0.1	1.3	0.3	0.1	1.3	0.3
L_p(mm)	0.5	4	0.5	0.5	4	0.5
α (°)	0	20	4	0	20	4

The EM full-wave simulations with the CST software are used for the collection of training and testing samples. The neural networks designed to predict the *S*-parameter are composed of two hidden layers with 10 and 30 neurons, respectively. The neural network designed to predict the gain has a single hidden layer consisting of 15 neurons. The four sub-ANNs for the prediction of the *S*-parameter and the sub-ANN for the prediction of the gain are trained with the Levenberg-Marquardt optimization algorithm with an initial learning rate of 0.001. All the networks are trained with a set of input parameters and their corresponding *S*-parameter or gain values. The training process based on the back propagation scheme iteratively adjusts the weights of all neurons until the desired accuracy level is achieved. The mean absolute percentage error (MAPE) is used to calculate the training and testing errors. The training MAPEs of the ANN model are 4.56% for $|S_{11}|$ and 3.45% for the gain, while the testing MAPEs are 5.62% for $|S_{11}|$ and 4.12% for the gain.

Once the training of ANN is completed, it can be repeatedly called by NSGA-II for the optimization of BAVA in place of the traditional full wave simulation. The optimized variables are $\boldsymbol{x} = (\Delta y_2, \Delta y_3, \Delta y_4, \Delta y_5, \Delta y_6, \Delta y_7, L_p, W_p, \alpha)$. The initial population, which includes 500 individuals, is randomly generated within the range of the variables shown in Table 1. The objective of optimization is to obtain the best possible *S*-parameters and gain. The final optimal structural parameters are as follows: $\boldsymbol{x}_{opt1}$ = (0 mm, -1.6 mm, 0.2 mm, -1.6 mm, 0.8 mm, 0.2 mm, 4 mm, 0.8 mm, 12°). Here, the optimal parameters of $\boldsymbol{x}_{opt1}$ are input to both the ANN model and the CST software to obtain the *S*-parameter and gain of BAVA. When the simulated results from the CST software are regarded as the benchmark, the MAPEs of the *S*-parameter and gain from the ANN model are 1.5% and 0.6%, respectively, indicating its high calculation accuracy.

To highlight the advantages of the proposed approach, we set Δy_k = 0 mm (k = 1,2, …,7) and get the straight slots for comparison. The results are shown in Fig. 5. After the optimization of the BAVA with the straight slots, the optimal structural parameters are as follows: $\boldsymbol{x}_{opt2}$ = (0 mm, 0 mm, 0 mm, 0 mm, 0 mm, 0 mm, 4 mm, 1.3 mm, 0°).

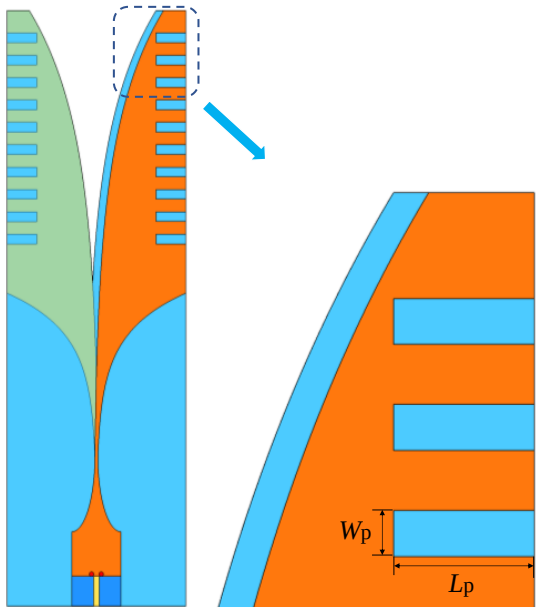

Fig. 5. BAVA with straight slots.

Figure 6 illustrates the simulated results of the BAVAs with the optimal structures of straight slots and curved slots. One can see from Fig. 6 that, the curved slots designed by the proposed model lead to a broader frequency band with nearly the same gain and cross-polarization levels as the straight slots in BAVA. According to Fig. 6 (a), the lower cut-off frequency of the BAVA with straight slots is 7.97 GHz, while that with curved

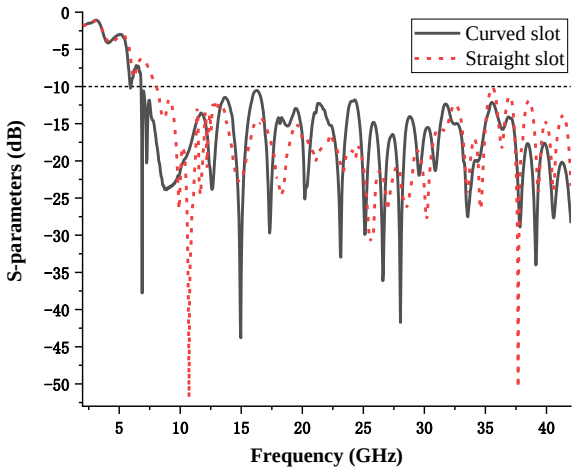

(a)

Fig. 6. *Continued*

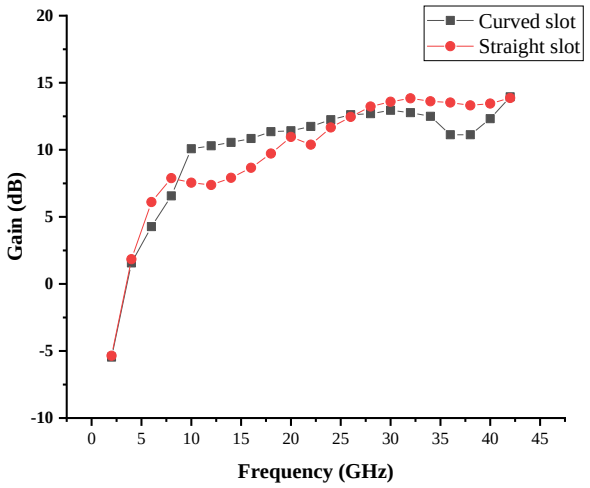

(b)

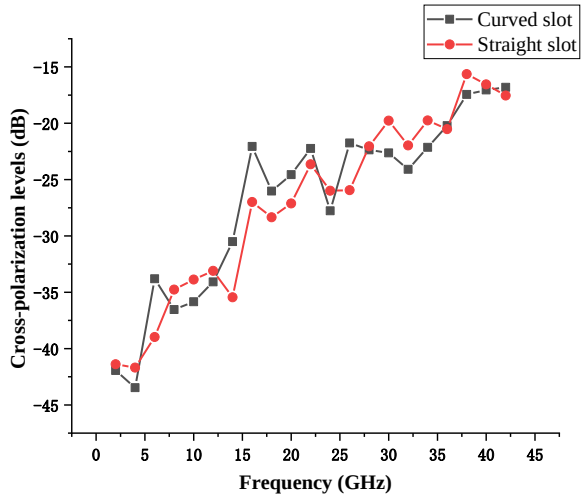

(c)

Fig. 6. Comparison of radiation performance between BAVAs with curved slots and straight slots: (a) $|S_{11}|$, (b) gain, and (c) cross-polarization level.

slots is 6.76 GHz. This indicates that the lower cut-off frequency of the BAVA with curved slots is reduced by about 1.2 GHz.

IV. CONCLUSION

In this paper, an ANN for parametric modeling based on cubic spline interpolation is proposed to shape the slots of BAVA. The longitudinal movement values of the points, rotation angle, width, and length of the curved slot serve as the input of ANN. These input parameters of ANN help to determine the slot structure. The output of the proposed ANN includes the *S*-parameter as well as the gain of the antenna. The lower cut-off frequency is decreased without affecting BAVA's gain, thanks to the curved slots created by the proposed ANN and further optimized by NSGA-II. The proposed ANN only involves simple geometric parameters instead of image processing, leading to a convenient operation of machine learning. Moreover, the parametric modeling can also be adapted to shape design of other devices.

ACKNOWLEDGMENT

This work was supported by the National Natural Science Foundation of China under Grant 62171093 and by the Sichuan Science and Technology Programs under Grants 2022NSFSC0547 and 2022ZYD0109.

REFERENCES

[1] F. T. Wu, G. F. Zhang, X. L. Yuang, and N. C. Yuang, "Research on ultra-wide band planar Vivaldi antenna array," *Microw. Opt. Technol. Lett.*, vol. 48, no. 10, pp. 2117-2120, Oct. 2006.

[2] M. J. Horst, M. T. Ghasr, and R. Zoughi, "Design of a compact V-band transceiver and antenna for millimeter-wave imaging systems," *IEEE Trans. Instrum. Meas.*, vol. 68, no. 11, pp. 4400-4411, Nov. 2019.

[3] M. R. Hamid, P. Gardner, P. S. Hall, and F. Ghanem, "Vivaldi with tunable narrow band rejection," *Microw. Opt. Technol. Lett.*, vol. 53, no. 5, pp. 1125-1128, May 2011.

[4] P. J. Gibson, "The Vivaldi aerial," in *Proc. 9th Eur. Microw. Conf.*, Brighton, U.K., pp. 101-105, June 1979.

[5] E. Gazit, "Improved design of the Vivaldi antenna," *IEE Proc. H-Microw. Antennas Propag.*, vol. 135, no. 2, pp. 89-92, Apr. 1988.

[6] J. D. S. Langley, P. S. Hall, and P. Newham, "Novel ultrawide-bandwidth Vivaldi antenna with low crosspolarisation," *Electron. Lett.*, vol. 29, no. 23, p. 2004, 1993.

[7] A. Dadgarpour, F. Jolani, Y. Yu, Z. Chen, B. S. Virdee, and T. A. Denidni, "A compact balanced antipodal bow-tie antenna having double notch-bands," *Microw. Opt. Technol. Lett.*, vol. 56, no. 9, pp. 2010-2014, Sep. 2014.

[8] M. C. Sai and D. Chandwani, "Balanced antipodal Vivaldi antenna design with hexagonal slots and three level geometric patches," in *2019 3rd International conference on Electronics, Communication and Aerospace Technology (ICECA)*, Coimbatore, India, pp. 1057-1060, June 2019.

[9] L. Juan, F. Guang, Y. Lin, and F. Demin, "A modified balanced antipodal Vivaldi antenna with improved radiation characteristics," *Micro & Optical Tech Letters*, vol. 55, no. 6, pp. 1321-1325, June 2013.

[10] Y.-F. Liu, L. Peng, and W. Shao, "An efficient knowledge-based artificial neural network for the design of circularly polarized 3-D-printed lens

antenna," *IEEE Trans. Antennas Propagat.*, vol. 70, no. 7, pp. 5007-5014, July 2022.

[11] T. N. Kapetanakis, I. O. Vardiambasis, M. P. Ioannidou, and A. Maras, "Neural network modeling for the solution of the inverse loop antenna radiation problem," *IEEE Trans. Antennas Propagat.*, vol. 66, no. 11, pp. 6283-6290, Nov. 2018.

[12] L.-Y. Xiao, W. Shao, F.-L. Jin, and B.-Z. Wang, "Multiparameter modeling with ANN for antenna design," *IEEE Trans. Antennas Propagat.*, vol. 66, no. 7, pp. 3718-3723, July 2018.

[13] L.-Y. Xiao, W. Shao, F.-L. Jin, B.-Z. Wang, and Q. H. Liu, "Inverse artificial neural network for multiobjective antenna design," *IEEE Trans. Antennas Propagat.*, vol. 69, no. 10, pp. 6651-6659, Oct. 2021.

[14] H.-Y. Luo, W. Shao, X. Ding, B.-Z. Wang, and X. Cheng, "Shape modeling of microstrip filters based on convolutional neural network," *IEEE Microw. Wireless Compon. Lett.*, vol. 32, no. 9, pp. 1019-1022, Sep. 2022.

[15] N.-N. Wang, M. Fang, H.-T. Chou, J.-R. Qi, and L.-Y. Xiao, "Balanced antipodal Vivaldi antenna with asymmetric substrate cutout and dual-scale slotted edges for ultrawideband operation at millimeter-wave frequencies," *IEEE Trans. Antennas Propagat.*, vol. 66, no. 7, pp. 3724-3729, July 2018.

Wen-Hao Su received the B.S. degree from the University of Electronic Science and Technology of China (UESTC), Chengdu, China, in 2021, where he is currently pursuing the master's degree in radio physics.

His current research interests include antenna design and computational electromagnetics.

Wei Shao received the B.E. degree in electrical engineering from UESTC in 1998, and received M.Sc. and Ph.D. degrees in radio physics from UESTC in 2004 and 2006, respectively.

He joined UESTC in 2007 and is now a professor there. From 2010 to 2011, he was a visiting scholar in the Electromagnetic Communication Laboratory, Pennsylvania State University, State College, PA. From 2012 to 2013, he was a visiting scholar in the Department of Electrical and Electronic Engineering, the University of Hong Kong. His research interests include computational electromagnetics and antenna design.

Haiyan Ou received the B.E. degree in electrical engineering from UESTC in 2000, and received Ph.D. degrees in optical engineering from Zhejiang University in 2009.

She joined UESTC in 2009 and is now an associate professor there. From 2010 to 2011, she was a visiting scholar in the department of Engineering, Cambridge University, UK. From 2012 to 2013, she was a post-doc in the Department of Electrical and Electronic Engineering, the University of Hong Kong. Her research interests include computational electromagnetics, microwave photonics, and digital holography.

Sheng-Jun Zhang received a Ph.D. in science from Beijing University of Technology in 2001. From then on he joined the team in National Key Laboratory of Science & Technology on Test Physics and Numerical Mathematics. He is now professor of the laboratory and his research interests include scattering of EM waves, EM effects of periodic structures such as FSS, PC, and gratings, as well as modulation of scattering of materials and interaction of EM waves with plasmas, and IR radiation management.

He has published some papers in journals and conferences, in addition to patents and two books.